

Changes in the time-space dimension of human mobility during the COVID-19 pandemic

Clodomir Santana¹, Federico Botta^{1,2}, Hugo Barbosa¹, Filippo Privitera³, Ronaldo Menezes^{1,2}, and Riccardo Di Clemente^{1,2*}

¹University of Exeter, Computer Science Department, Exeter, EX4 4QF, United Kingdom

²The Alan Turing Institute, London, NW1 2DB, United Kingdom

³Cuebiq Inc., Milan, Italy

*corresponding author: r.di-clemente@exeter.ac.uk

ABSTRACT

Socio-economic constructs and urban topology are crucial drivers of human mobility patterns. During the COVID-19 pandemic, these patterns were re-shaped in their main two components: the spatial dimension represented by the daily travelled distance, and the temporal dimension expressed as the synchronisation time of commuting routines. Leveraging location-based data from de-identified mobile phone users, we observed that during lockdowns restrictions, the decrease of spatial mobility is interwoven with the emergence of asynchronous mobility dynamics. The lifting of restriction in urban mobility allowed a faster recovery of the spatial dimension compared to the temporal one. Moreover, the recovery in mobility was different depending on urbanisation levels and economic stratification. In rural and low-income areas, the spatial mobility dimension suffered a more significant disruption when compared to urbanised and high-income areas. In contrast, the temporal dimension was more affected in urbanised and high-income areas than in rural and low-income areas.

Introduction

The places we visit^{1–3}, the products we purchase^{4–6}, the people we interact with^{7–9}, among others activities, produce digital records of our daily activities. Once decoded and analysed, this digital fingerprint provides a new ground to portray urban dynamics^{10,11}. In particular, the sequence of locations gathered from mobile phone devices via Calls Detail Records (CDR) and Location-Based Service data (LBS) offers a unique opportunity to assess a broad time span of people's urban activities in almost real-time, overcoming the limitations of surveys and censuses^{12,13}. CDR and LBS give us information about people's daily motifs across urban locations¹⁴, their attitude in exploring different places¹⁵, the route of their commutes^{16,17} and the purpose of their urban journey¹⁸. The location of people in cities is predictable¹⁹, and is strictly connected with the circadian rhythms of social activities²⁰, as well as home and work locations. The spatio-temporal variability of commuting patterns²¹ is intertwined with the mode of journey²², the population density (i.e. urbanisation level)²³ and the socio-economic status^{24–26}.

CDR and LBS contribute to the continuous creation of snapshots of citizens' mobility patterns and represent a needed instrument to provide valuable insights on population dynamics in circumstances that urge rapid response^{27,28}. They have been used to inform public health policymakers assessing the spread of a disease across the population^{29–31}. Recently, during the COVID-19 pandemic, LBS metrics have become a proxy to evaluate the effectiveness and effects of mobility restriction policies enforced by local governments worldwide^{32–35}. Using aggregated mobility data, researchers around the world can develop models to study and predict transmission dynamics^{36–38}, investigate the impact and effectiveness of restriction policies, and re-opening strategies^{38–45,45–47}, and analyse the effects of these policies on the local economy, ethnic and socio-economic groups^{48–51}. Moreover, coupling the mobility data with the socio-economic and ethnicity groups from the census, it is possible to estimate the socio-economic impact of such restrictions in each different community^{52–56}.

Although many studies are tackling the changes in human mobility patterns during the COVID-19 pandemic, most of them focus on the changes in the spatial dimension of the mobility, i.e. if the citizens are changing the patterns of their whereabouts in terms of magnitude (radius of gyration⁵⁷ and/or the location visited⁴⁷). The temporal analysis of the commuting pattern integrated into the calculation of the mobility metric is missing from the COVID-19 literature. Since urban mobility patterns are built upon the space and the time dimension⁵⁸, it is vital also to study the temporal dimension of mobility during the pandemic.

We can assess the space-time interaction⁵⁹ of human activities, studying the rhythms of human mobility with the spatial span of the urban whereabouts. The challenge at hand is to disentangle and investigate how each dimension have been reshaped

during the pandemic. To assess the changes in the spatial mobility patterns, preserving citizen privacy under the GDPR¹, we employ the radius of gyration^{60,61} as a spatial metric. To calculate the extent of the urban movement, we used mobility synchronisation as a time metric that quantifies the co-temporal occurrence of the daily mobility motifs. In the context of the pandemic, these two dimensions are of fundamental interest in a sense that they capture how far infectious individuals could potentially travel and how many people they could be in contact with (e.g., public transport, office spaces).

Leveraging LBS data from de-identified mobile phone users who opted-in to anonymous location sharing for research purposes, we study how citizen mobility patterns changed from January 2019 to February 2021 across the UK. We disentangled how each mobility dimension has been affected by the pandemic and the adopted policies to mitigate its impact. At the lifting of each restriction, the spatial mobility dimension recovered faster than the temporal dimension. The space-time components drift their trends during the second lockdown to finally align back after the third lockdown.

We coupled the mobility dimensions with the urbanisation, unemployment, occupation, and income levels from the census at the local authorities level. Rural and urban areas manifest opposite trends. In rural areas, the lockdowns affect more the spatial dimension, where the locations of human activities are spread apart and consequently the trips a longer². Meanwhile, in urbanised areas, the synchronicity of the daily activity was dissolved possibly by the rise of asynchronous commuting patterns (e.g. flexible work hours or rotational/staggered shifts)^{62,63}.

We observed that, during the pandemic, the unemployment rates affect more the temporal dimension than the spatial one, where high unemployment levels were associated with low mobility synchronisation. Moreover, this effect seems to be tied with the urbanisation level of the local authorities. Lastly, we adopt the national statistics socio-economic classification (NS-SEC) as a proxy to gauge the impact of the pandemic on the mobility patterns of income/occupation groups. We noticed that areas with elevated concentration of population on low-income routine occupations had the most significant reduction in the spatial and temporal dimensions of mobility.

Results

Throughout this section, we define the spatial dimension of human mobility as the span of the citizen's movement, i.e. the length of the trips. This dimension is gauged using the radius of gyration, which quantifies *how far* from the centre of a user's mobility the visited geographical locations are spread. In the temporal dimension, we are interested in measuring co-temporal events linked to collective, synchronised behaviours. This dimension is estimated with the mobility synchronisation metric that represents temporal regularities related to *when* people tend to leave their residences at regular time period. Our goal is to quantify how containment measures (e.g., limited social gatherings, business and schools closures, home working) affected travel rhythms of the populations. The intervals are identified through the analysis of the strongest frequency components in Fourier spectra of the *out-of-home trips* time series. More information on these metrics is available in the Methods section.

We analysed LBS data from January 2019 to February 2021 in the UK. This period includes the three lockdowns announced by the UK's prime minister³. Given the discrepancies in the implementation of the different lockdown across each country in the UK, an analysis of the local/regional impact of the pandemic is included in the Supporting Information: Northern Ireland (Fig. S5.10 and Fig. S5.11), Scotland (Fig. S6.12 and Fig. S6.13), Wales (Fig. S7.14 and Fig. S7.15) and England (Fig. S4.8 and Fig. S4.9).

Fig. 1 depicts the radius of gyration and mobility synchronisation trends from week 2 of 2020 to week 7 of 2021. Both metrics have similar trends up to week 18 of 2020 when the radius starts recovering to pre-pandemic levels while the synchronisation does not. The recovery in the spatial dimension coupled with the fluctuations in the temporal patterns suggests that, although people gradually started making trips similar to the period before the pandemic, these trips do not present the temporal synchronisation observed before. After the third lockdown, we can notice similar trends in the spatial and temporal dimensions as in the period before week 18.

Since mobility synchronisation measures the existing time trends, it can estimate the effects of human mobility restrictions policies, such as lockdowns. We can see reductions in the mobility synchronisation levels during all three lockdowns. However, the second one produced the most significant decrease in the synchronicity levels in most local authorities compared to the other two; 78.34% of the local authorities experienced a reduction in the synchronisation level compared to the baseline. In contrast, during the first and the third lockdown, the mobility synchronisation decreased in 56.67% and 34.02% of the local authorities, respectively. The expressive drop in the mobility synchronisation during the second lockdown might be tied to the changes in the *stay-at-home* policy³.

Human mobility patterns are also affected by urbanisation level⁶⁴. For example, rural areas are characterised by limited accessibility to goods, services and activities⁶⁵. In the context of a pandemic, the urbanisation level partly explains differences in mobility patterns⁶⁶, and the diffusion of infectious diseases⁶⁷⁻⁶⁹.

¹General Data Protection Regulation, more information available at gdpr-info.eu/

²Data from National Travel Survey: England 2018, available at gov.uk/government/statistics/national-travel-survey-2018

³GOV.UK: Coronavirus press conferences, available at gov.uk/government/collections/slides-and-datasets-to-accompany-coronavirus-press-conferences

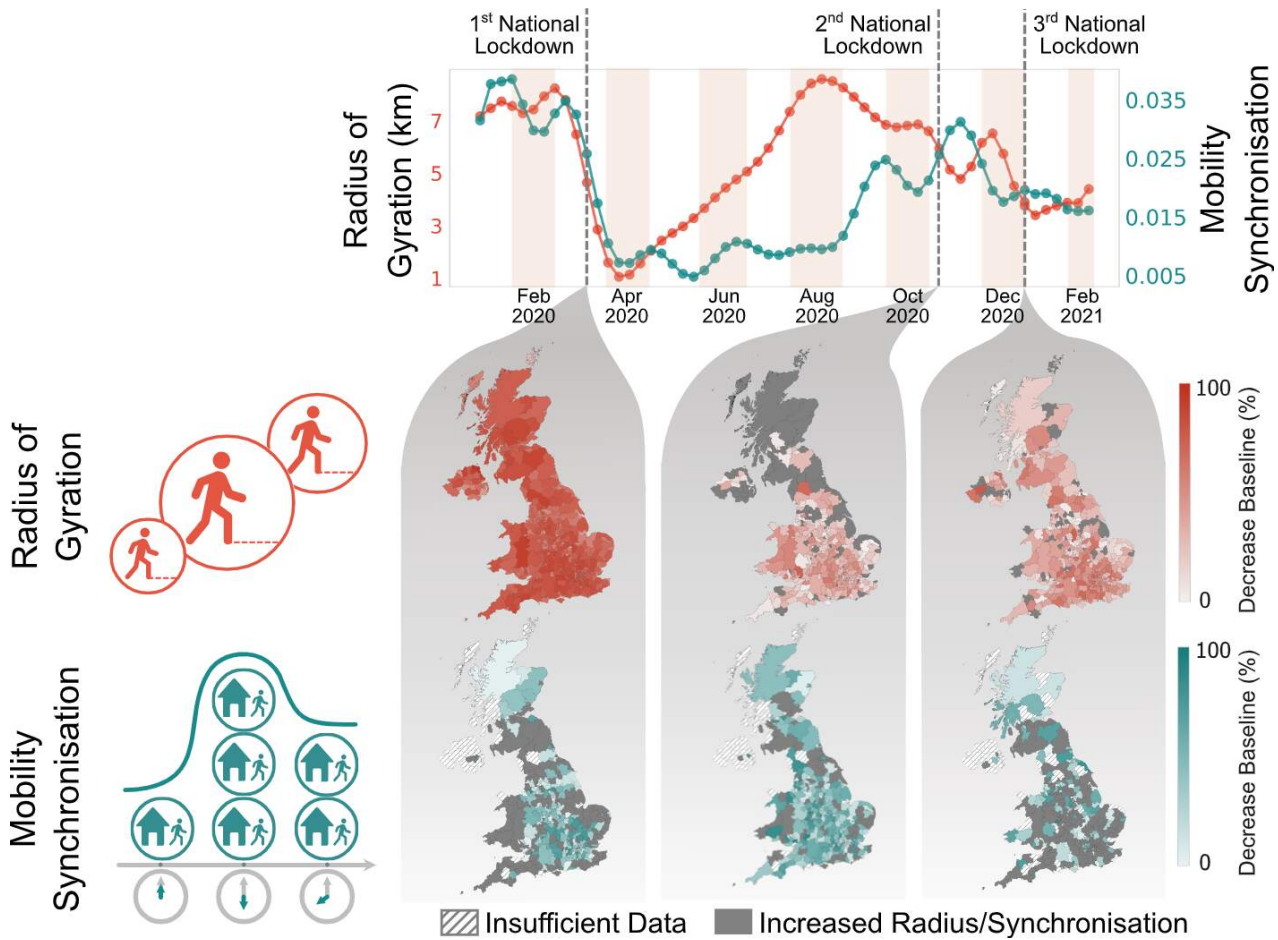


Figure 1. Evolution of the radius of gyration and mobility synchronisation in the UK's local authorities from the second week of 2020 to week 7 of 2021. The maps depict the effects of the three English national lockdowns regarding the spatio-temporal metrics adopted. Note that the first lockdown resulted in the most significant reduction in the radius of gyration in all four nations. However, it is worth mentioning that the first lockdown was the only one with the same restrictions for all UK's countries. Concerning mobility synchronisation, the most notable reduction occurred during the second lockdown. Additionally, it is challenging to disentangle the effects of the third lockdown from the changes in the population mobility patterns caused by end-of-year holidays.

To assess how the spatio-temporal mobility patterns of areas with different levels of urbanisation were affected during the COVID-19 pandemic, we analyse the radius of gyration and mobility synchronisation by urbanisation level. We divided the local authorities into three classes accordingly to the urban-rural classification adopted for England⁷⁰ illustrated in Fig 2 A.

We employed the concept of residual activity⁶⁰ to visualise the deviations of the mobility patterns during the lockdowns when compared to their expected behaviour (e.g. we used the same period of 2019 as the baseline for comparisons). Figure 2 B depicts the different responses of the urban-rural group to the three national lockdowns. High residual values indicate an increased number of trips compared to the expected behaviour (baseline period).

During the first lockdown, urban areas presented an increase in expected mobility. In contrast, rural areas have a negative trend. However, during the second and third lockdown, an opposite scenario emerges. Rural local authorities increased the expected residual activity, and urban areas decreased it. These differences can be driven by the change in the mobility restriction policies and the characteristics and pre-existing social vulnerabilities of urban and rural areas, as found in previous works⁷¹.

Although there is a debate as to whether a high population density accelerates or not the spread of the virus⁷², other urban and rural characteristics can be risk factors for COVID-19. For example, transportation systems and increased inter/intra urban connectivity are regarded as key factors contributing to the spread of contagious diseases⁷³.

The results of the radius of gyration (Fig. 2 C) and the mobility synchronisation (Fig. 2 D) also indicate differences in the

response of urban and rural areas to the lockdowns. Due to the characteristics of the geographic distribution of local amenities in rural areas, people tend to have a greater radius of gyration compared to urban areas⁴.

Analysing the trends of the radius of gyration and mobility synchronisation compared to the baseline of 2019, we can notice some differences in the urban-rural and spatio-temporal response of the local authorities (scatter plots on Fig 2 C and D). In the spatial dimension, we can see the same behaviour for urban and rural areas, characterised by a reduction in the mobility levels in the week before and the first week of lockdown. The shift between the baseline and the first/second lockdown indicates that the radius during the first week was significantly smaller than the week before these lockdowns.

In the temporal dimension, however, the differences between the mobility levels in the week before the lockdown and the first week of lockdown (first scatter plot in Fig. 2 D) are less dramatic than observed in the spatial dimension. Nonetheless, compared to the baseline, we can still see a reduction in the synchronisation values for urban and rural areas, especially in the second and third lockdowns (baseline plot in Fig. 2 D).

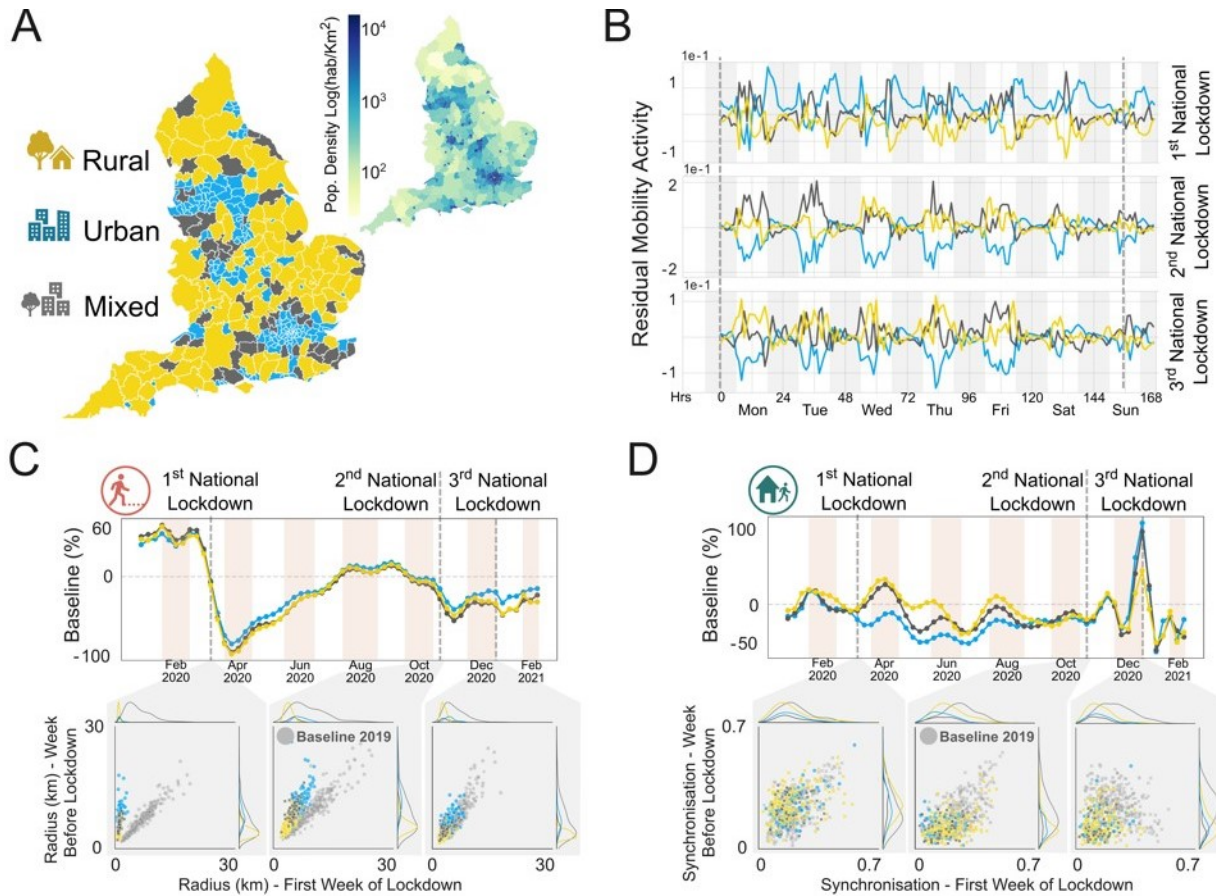


Figure 2. Radius of gyration and mobility synchronisation of English local authorities grouped according to the Urban-Rural classification (A). Panel (B) compares the differences in the number of out-of-home trips for the different urban-rural groups. Notice that after the first lockdown, urban local authorities started to present negative values in their curve. Panels (C) and (D) illustrate, respectively, a time series with variations on the radius of gyration and mobility synchronisation when compared to the baseline year (2019).

As discussed, the number of trips has decreased across all the urban-rural groups during the pandemic (Fig. S3.3). Because work-related activities often create the necessity to leave home, the rise in home-working and unemployment rate contribute to the reduction in the mobility levels⁷⁴. Next, we study the relationship between the spatio-temporal mobility metrics and the unemployment rate for areas with different levels of urbanisation, both before and during the pandemic. We estimate the size of the unemployed population based on the unemployment claimant count⁵.

We divided the time series of the radius of gyration and mobility synchronisation into pre-pandemic (from April 2019

⁴Data from National Travel Survey: England 2018, available at gov.uk/government/statistics/national-travel-survey-2018

⁵Data from the Office for National Statistics, available at ons.gov.uk/employmentandlabourmarket/peoplenotinwork/unemployment/datalist?filter=datasets

to February 2020) and pandemic (from April 2020 to February 2021) periods, and we analysed the Kendall Tau correlation between them and unemployment claimant count.

At first glance, the positive correlation between the radius of gyration and the unemployment rate seems to be dissonant from previous works^{12,25}. However, this result can be due to a rise in the unemployment rate and the spatial mobility levels before the pandemic (See SI Fig. S3.3). For the pandemic period, although the lockdowns have reduced the radius during specific periods, we see in Fig. 1 a period between April and August 2020 when the radius increased, making the correlation positive.

While the correlation between the spatial dimension of mobility and unemployment drops only marginally, preserving the positive sign and affecting more urban than rural areas, the correlation between the time dimension of mobility and unemployment drops significantly, becoming negative and impacting more rural districts than the urban.

The same explanation applies to mobility synchronisation in the pre-pandemic period. During the pandemic, we can see that the spatio-temporal dimensions display different patterns between May and November, and the temporal one does not present the same steep recovery as the spatial between April and August 2020. The oscillations in the patterns of the temporal dimension impacted the correlation with unemployment, making it negative.

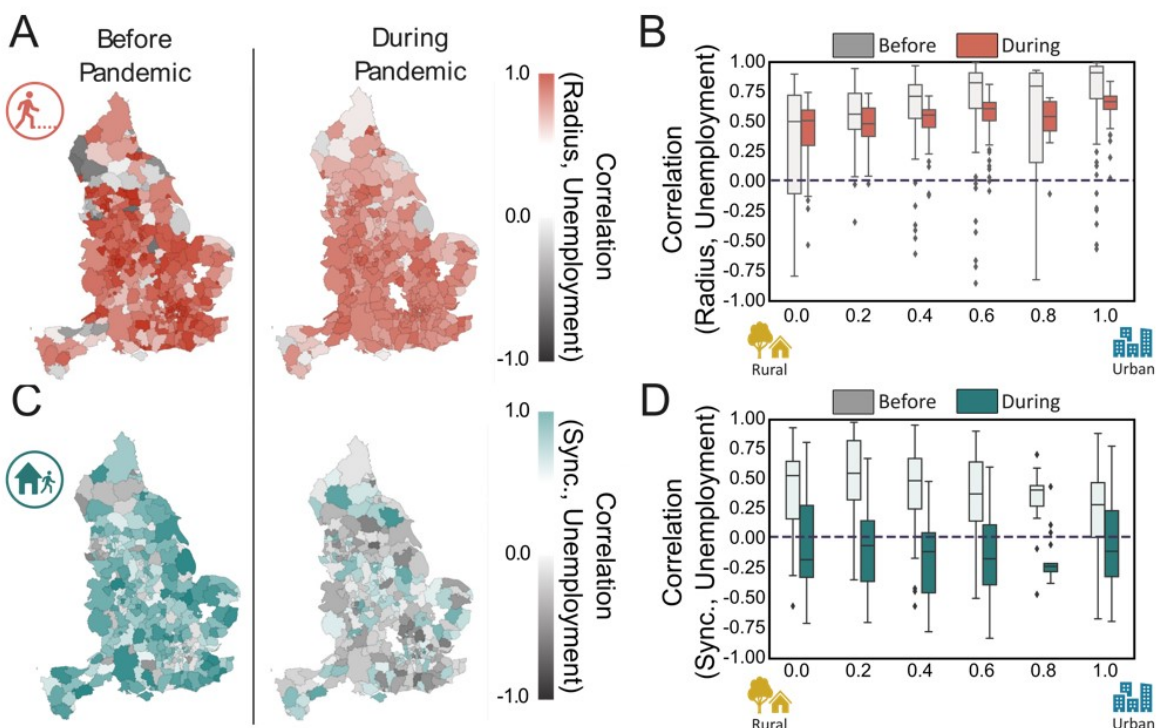


Figure 3. Correlation between the spatio-temporal metrics of human mobility and the unemployment claimant count. Panel A and C look at, respectively, the correlation between the radius of gyration and mobility synchronisation with the unemployment claimant count for the periods before and during the pandemic. Notice that, before the pandemic, both the radius and the synchronisation positively correlated with the unemployment claimant count. However, during the pandemic, the correlation with the radius became less strong, and that with synchronisation became negative. It is also worth mentioning that panels B and D reveal a possible association between correlation changes and areas' urbanisation level.

We argued that work trips contribute to the creation of our mobility patterns. Moreover, the type of occupation, among other socio-demographic characteristics, also influences those patterns⁷⁵. In this sense, we use the English National Statistics Socio-economic classification (NS-SEC)⁶ to gauge the response of employment relations and conditions of occupations to the pandemic. Using this classification, we also have insights into the connection between the spatio-temporal mobility and wealth level. The local authorities' population concentration in each NS-SEC class can be found in Supplementary Materials Fig. S2.2. This analysis is important since wealth and economic segregation are linked to differences in mobility patterns and response to human mobility restrictions under COVID-19 pandemic³³.

⁶The National Statistics Socio-economic Classification, available at ons.gov.uk

In the NS-SEC classification, classes related to managerial occupations exhibit strong positive correlation with income as depicted in Fig. 4 A. In contrast, lower supervisory, technical, semi-routine or routine occupations negatively correlate with income. The remainder of NS-SEC classes does not aggregate a diverse range of occupations. However, they do present a strong correlation with income.

Moreover, Fig. 4 B shows that, before and during the COVID-19 pandemic, people's radius of gyration and the mobility synchronisation within an area tend to grow as the concentration of population in managerial occupations increases. The opposite result is observed when analysing the percentage of the population (quartiles Q1 to Q4) in lower supervisory, semi-routine or routine occupations.

In all scenarios depicted in Fig. 4, we can see a reduction in the temporal and spatial dimensions of mobility during the pandemic. However, each group contributed differently to the overall change in the mobility observed during the pandemic. As mentioned before, the first national lockdown produced the most significant impact on the spatial dimension of mobility. In contrast, the second greatly impacted the temporal dimension.

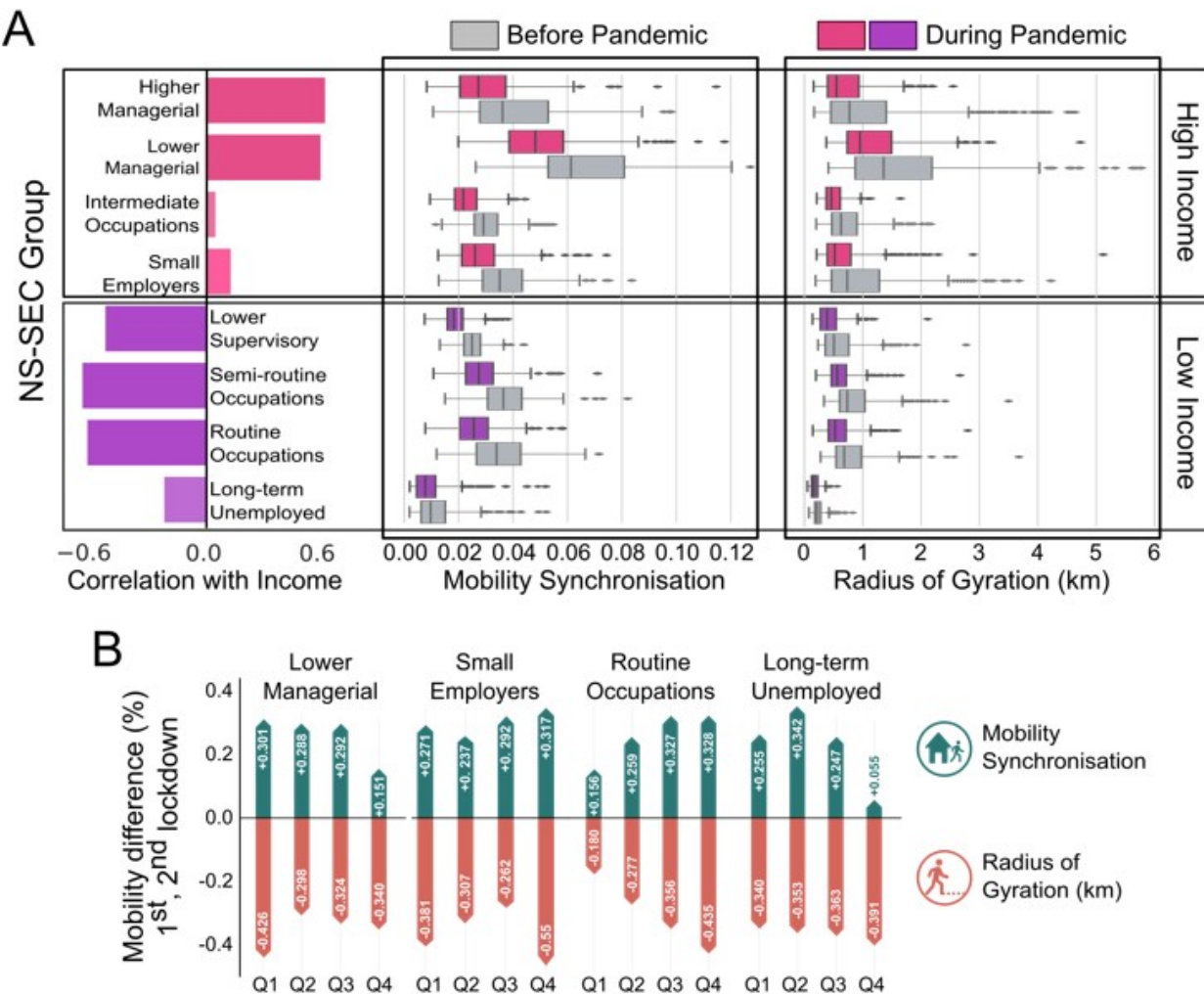


Figure 4. Relation between the NS-SEC classification, income and their impact on the spatio-temporal mobility patterns before and during the pandemic. Panel A looks at the correlation between the NS-SEC classes and the population income. In this panel, the classes coloured in pink and purple have positive and negative correlations with the population income. Panel A also shows the radius of gyration/mobility synchronisation of each NS-SEC class before and during the pandemic. Lastly, panel B highlights the differences between the first and second lockdowns in the spatio-temporal metrics.

Discussion

The accurate estimation of spatio-temporal facets of human mobility and gauging its changes as a reflection of the pandemic and mobility restriction policies is critical for assessing the effectiveness of these policies and mitigating the spread of COVID-19. A vital contribution of our work lies in applying two metrics to disentangle the changes in mobility's temporal and spatial dimensions. Using the radius of gyration, we could identify that the effect of the first lockdown was more significant than the other ones in changing the spatial characteristics of citizens' movement. Among the reasons that could lead to this result, we can mention more strict policies adopted in the first lockdown and the lockdown duration. However, further investigation is needed to obtain more pieces of evidence to support these hypotheses.

In contrast to the spatial dimension of mobility, the results indicate that the temporal one was more impacted during the second lockdown when more flexible mobility restriction policies were enforced. After the first lockdown, we argue that people who could not work from home were allowed to leave home and work in the office as long as they respected social distancing rules. Different work shifts were created to comply with these rules and limit the number of people inside indoor spaces. As a result, instead of having the same, or similar, work schedule for all employees, they started to be divided into groups that should go on different days of the week and at different times, impacting the temporal synchronisation of their movement.

Besides the changes during different periods and under different mobility restriction policies, we also analysed the interplay between the characteristics of the area (e.g. level of urbanisation, income and unemployment rates) and the spatio-temporal human mobility metrics adopted. We noticed that rural areas presented a more significant reduction in spatial patterns compared to urban ones. At the same time, urban areas were more impacted in their temporal dimension than rural ones. These differences observed in the urban-rural classification are correlated to the population density of the regions and can affect the impact of the mobility restriction measures.

We also observed changes in the response of regions regarding their unemployment rates and populations income. For the unemployment rates, we observed that before the COVID-19 pandemic, the unemployment claimant count was positively correlated with the radius of gyration and mobility synchronisation in the majority of the areas. However, during the pandemic, this correlation became weaker for the radius of gyration and negative for mobility synchronisation. Less urbanised areas tend to have a lower spatial correlation and a higher temporal correlation with unemployment than more urbanised areas. Using the NS-SEC classification as a proxy to assess the response of different income and work groups, we observed that low-income routine/semi-routine occupations were the groups that presents the greatest reduction in their radius and synchronisation. Moreover, the changes in the mobility restriction policies after the first lockdown had an impact on these groups, which can be the reason behind the greatest impact on the temporal dimension of mobility.

In summary, the analysis of the spatial dimension of human mobility coupled with the insights from the study of the temporal dimension allows us to characterise the impact of policies such as *stay-at-home* and school closures on the population of different areas/socioeconomics. These differences suggest that each group experiences, in a particular way, the emergence of asynchronous mobility patterns primarily due to the enforcement of mobility restriction policies and the ascension of new habits (e.g. home office and home education).

Methods

Data Sources

Human Mobility Data

Cuebiq Inc provided the human mobility data used in this research for research purposes. This data was collected from anonymous mobile phone users who have opted-in to give access to their location data anonymously, through a GDPR-compliant framework. Researchers queried the mobility data through an auditable, cloud-hosted sandbox environment, receiving aggregate outputs in return. The datasets contain records of UK users from January 2019 to early March 2021. In total, we have over 17.8 billion Out-of-home trips and about 1 billion users' radius of gyration records. Note that the radius logs are measured on a weekly basis while the trips are recorded on a daily basis. More information on the datasets is available in the SI. We assessed the representativeness of the data by analysing the correlation between the number of users and the population of the local authorities. A strong positive correlation between the populations compared with r^2 value equal to 0.78 was obtained (see the Supporting Information Fig. S1.1). The data is composed of records of when users leave the area (as a square of 500m) that is related to their homes and the length of the trips. The home area is estimated based on the history of places visited, the amount of time spent at the area and the period when the user stayed at the location following^{21,76}. Due to the composition of our data set, we currently cannot perform analysis related to points of interest (POI), for instance.

Other Data Sources

The Income study employed data from the report on income estimates for small areas in England in 2018 provided by the Office for National Statistics (ONS)⁷⁷. It is available for download and distribution under the terms of the Open Government Licence

⁷. Similarly, the analysis of the unemployment claimant rate, the urban-rural classification of English local authorities⁷⁰ and the national statistics socio-economic classification⁷⁸ used the data published by the ONS publicly available under the terms of the Open Government Licence. The remaining socioeconomic data utilised aggregated data from the UK Census of 2011⁷⁹, which is available for download at the InFuse platform also under the terms of the Open Government Licence.

Metrics and Other Methods

Radius of Gyration

We conducted the study of the radius of gyration (RG) following the definition of Gonzalez et al.⁶⁰. It can be described as the characteristic distance travelled by a user u during a period and is calculated as follows

$$RG_u = \sqrt{\frac{1}{N_u} \sum_{i=1}^{N_u} (\vec{r}_u^i - \vec{r}_u^{cm})^2} \quad (1)$$

where, N_u represents the unique locations visited by the user, \vec{r}_u^i is the geographic coordinate of location i and \vec{r}_u^{cm} indicates the centre of mass of the trajectory calculated by

$$\vec{r}_u^{cm} = \frac{1}{N_u} \sum_{i=1}^{N_u} n_u^i \vec{r}_u^i \quad (2)$$

where n_u^i is the visit frequency or the waiting time in location i . The mobility value of each region is the median value of the radius of gyration of the users within a temporal window of 8 days centred around a given day.

Residual Mobility Activity

The concept of residual mobility activity displayed in Fig. 2 B was adapted from⁸⁰, and it is used to highlight differences between the measured behaviour of the local authorities compared to their expected behaviour. For a given local authority i is calculated as follows

$$a_i^{res}(t) = a_i^{norm}(t) - a^{-norm}(t) \quad (3)$$

where $a^{-norm}(t)$ is the normalised activity averaged over all local authorities under at each particular time, and $a_i^{norm}(t)$ is computed similarly to the Z-score metric

$$a_i^{norm}(t) = \frac{a_i^{abs}(t) - \mu^{abs}}{\sigma^{abs}} \quad (4)$$

where $a_i^{abs}(t)$ is the activity in a local authority at a specific time t , μ^{abs} is the mean activity of all local authorities under the same urban-rural classification of i at a specific time, and σ^{abs} represents the standard deviation of all local authorities under the same urban-rural classification of $a_{i,j}$ at a particular time.

Mobility Synchronisation

The mobility synchronisation is not limited to conventional commuting routines. It can happen at any time of the day in which people tend to perform certain activities. For example, school teachers, healthcare professionals, and other routine or semi-routine occupations tend to have defined times reserved for specific activities (e.g., eating, exercising, socialising). To have a more accurate portrait of the mobility synchronisation patterns, instead of analysing it as a concentration of trips around certain hours, we define the mobility synchronisation as the total magnitude in the periodicity in the out-of-home trips. An example of out-of-home trips for the baseline year is depicted in Fig. S3.7.

First, using 2019 as a baseline, we analyse the Wavelet and Fourier spectra to determine the expected strongest frequency components in the mobility regularity. For a given mother wavelet $\psi(t)$, the discrete wavelet transform can be described as

$$\psi_{j,k}(t) = \frac{1}{\sqrt{2^j}} \psi\left(\frac{t - k2^j}{2^j}\right) \quad (5)$$

⁷<http://www.nationalarchives.gov.uk/doc/open-government-licence/version/2>

where j and k are integers that represent, respectively, the scale and the shift parameters. For the Fourier transform, a discrete transform of the signal x_n , for $n = 0 \dots N - 1$ is:

$$X_k = \sum_{n=0}^{N-1} x_n e^{-i2\pi kn/N} \quad (6)$$

where $K = 0 \dots N - 1$ and $e^{-i2\pi kn/N}$ represents the *Nth roots of unity*.

Employing these two transforms, we found that the mobility patterns are characterised by five main periods, namely 24h, 12h, 8h, and 6h (see SI material Fig. S3.4). However, because the 24h component overshadows the other three components (see Fig. S3.6), we focus the analysis on the 12h, 8h, and 6h periods. Moreover, during the pandemic, these periods were more affected than the 24hrs component (see Fig. S3.5). Next, the mobility synchronisation metric is defined as the sum of the powers from the Lomb-Scargle periodograms⁸¹ corresponding to the 12h, 8h and 6h. The generalised Lomb-Scargle periodograms is calculated as

$$P_N(f) = \frac{1}{\sum_i y_i^2} \left\{ \frac{[\sum_i y_i \cos \omega(t_i - \tau)]^2}{\sum_i \cos^2 \omega(t_i - \tau)} + \frac{[\sum_i y_i \sin \omega(t_i - \tau)]^2}{\sum_i \sin^2 \omega(t_i - \tau)} \right\} \quad (7)$$

where y_i represents the N-measurements of a time series at time t_i , ω is a frequency, τ can be obtained from

$$\tan 2\omega\tau = \frac{\sum_i \sin 2\omega t_i}{\sum_i \cos 2\omega t_i} \quad (8)$$

The mobility synchronisation is a value between 0 and 1, where higher values for a given period indicate that more people left their homes simultaneously. In the context of the pandemic, high mobility synchronisation can be translated into a potential increase in the likelihood of being exposed or exposing more people to the virus due to the large number of people moving simultaneously.

References

1. Bohannon, J. Tracking People's Electronic Footprints, DOI: <https://doi.org/10.1126/science.314.5801.914> (2006).
2. Andrade, T., Cancela, B. & Gama, J. Discovering locations and habits from human mobility data. *Annals Telecommun.* **75**, 505–521, DOI: <https://doi.org/10.1007/s12243-020-00807-x> (2020).
3. Botta, F., Moat, H. S. & Preis, T. Quantifying crowd size with mobile phone and Twitter data. *Royal Soc. Open Sci.* **2**, DOI: <https://doi.org/10.1098/rsos.150162> (2015).
4. Xu, S., Di Clemente, R. & González, M. C. Mining urban lifestyles: Urban computing, human behavior and recommender systems. In *Big Data Recommender Systems: Application Paradigms*, 71–81, DOI: https://doi.org/10.1049/PBPC035G_ch5 (Institution of Engineering and Technology, 2019).
5. de Montjoye, Y.-A., Radaelli, L., Singh, V. K. & Pentland, A. S. Unique in the shopping mall: On the reidentifiability of credit card metadata. *Science* **347**, 536–539, DOI: <https://doi.org/10.1126/science.1256297> (2015).
6. Bannister, A. & Botta, F. Rapid indicators of deprivation using grocery shopping data. *Royal Soc. Open Sci.* **8**, DOI: <https://doi.org/10.1098/rsos.211069> (2021).
7. Candia, J. *et al.* Uncovering individual and collective human dynamics from mobile phone records. *J. Phys. A: Math. Theor.* **41**, 224015, DOI: <https://doi.org/10.1088/1751-8113/41/22/224015> (2008).
8. Gao, S., Liu, Y., Wang, Y. & Ma, X. Discovering Spatial Interaction Communities from Mobile Phone Data. *Transactions GIS* **17**, 463–481, DOI: <https://doi.org/10.1111/tgis.12042> (2013).
9. Eagle, N., Pentland, A. & Lazer, D. Inferring friendship network structure by using mobile phone data. *Proc. Natl. Acad. Sci.* **106**, 15274–15278, DOI: <https://doi.org/10.1073/pnas.0900282106> (2009).
10. “Sandy” Pentland, A. The Data-Driven Society. *Sci. Am.* **309**, 78–83, DOI: <https://doi.org/10.1038/scientificamerican1013-78> (2013).
11. Lazer, D. *et al.* Computational Social Science. *Science* **323**, 721–723, DOI: <https://doi.org/10.1126/science.1167742> (2009).

12. Toole, J. L. *et al.* The path most traveled: Travel demand estimation using big data resources. *Transp. Res. Part C: Emerg. Technol.* **58**, 162–177, DOI: <https://doi.org/10.1016/j.trc.2015.04.022> (2015).
13. Jiang, S. *et al.* The TimeGeo modeling framework for urban mobility without travel surveys. *Proc. Natl. Acad. Sci.* **113**, E5370–E5378, DOI: <https://doi.org/10.1073/pnas.1524261113> (2016).
14. Schneider, C. M., Belik, V., Couronné, T., Smoreda, Z. & González, M. C. Unravelling daily human mobility motifs. *J. The Royal Soc. Interface* **10**, 20130246, DOI: <https://doi.org/10.1098/rsif.2013.0246> (2013).
15. Pappalardo, L. *et al.* Returners and explorers dichotomy in human mobility. *Nat. Commun.* **6**, 8166, DOI: <https://doi.org/10.1038/ncomms9166> (2015).
16. Xu, Y., Di Clemente, R. & González, M. C. Understanding vehicular routing behavior with location-based service data. *EPJ Data Sci.* **10**, 12, DOI: <https://doi.org/10.1140/epjds/s13688-021-00267-w> (2021).
17. Kalila, A., Awwad, Z., Di Clemente, R. & González, M. C. Big Data Fusion to Estimate Urban Fuel Consumption: A Case Study of Riyadh. *Transp. Res. Rec. J. Transp. Res. Board* **2672**, 49–59, DOI: <https://doi.org/10.1177/0361198118798461> (2018).
18. Jiang, S., Ferreira, J. & Gonzalez, M. C. Activity-Based Human Mobility Patterns Inferred from Mobile Phone Data: A Case Study of Singapore. *IEEE Transactions on Big Data* **3**, 208–219, DOI: <https://doi.org/10.1109/TBDA.2016.2631141> (2017).
19. Song, C., Qu, Z., Blumm, N. & Barabási, A.-L. Limits of Predictability in Human Mobility. *Science* **327**, 1018–1021, DOI: <https://doi.org/10.1126/science.1177170> (2010).
20. Aubourg, T., Demongeot, J. & Vuillerme, N. Novel statistical approach for assessing the persistence of the circadian rhythms of social activity from telephone call detail records in older adults. *Sci. Reports* **10**, 21464, DOI: <https://doi.org/10.1038/s41598-020-77795-4> (2020).
21. Kung, K. S., Greco, K., Sobolevsky, S. & Ratti, C. Exploring Universal Patterns in Human Home-Work Commuting from Mobile Phone Data. *PLoS ONE* **9**, e96180, DOI: <https://doi.org/10.1371/journal.pone.0096180> (2014).
22. Wang, P., Fu, Y., Liu, G., Hu, W. & Aggarwal, C. Human Mobility Synchronization and Trip Purpose Detection with Mixture of Hawkes Processes. In *Proceedings of the 23rd ACM SIGKDD International Conference on Knowledge Discovery and Data Mining*, vol. Part F1296, 495–503, DOI: <https://doi.org/10.1145/3097983.3098067> (ACM, New York, NY, USA, 2017).
23. Yuan, Y. & Raubal, M. Extracting Dynamic Urban Mobility Patterns from Mobile Phone Data. In *Lecture Notes in Computer Science (including subseries Lecture Notes in Artificial Intelligence and Lecture Notes in Bioinformatics)*, vol. 7478 LNCS, 354–367, DOI: https://doi.org/10.1007/978-3-642-33024-7_26 (Springer, 2012).
24. Di Clemente, R. *et al.* Sequences of purchases in credit card data reveal lifestyles in urban populations. *Nat. Commun.* **9**, 3330, DOI: <https://doi.org/10.1038/s41467-018-05690-8> (2018).
25. Pappalardo, L., Pedreschi, D., Smoreda, Z. & Giannotti, F. Using big data to study the link between human mobility and socio-economic development. In *2015 IEEE International Conference on Big Data (Big Data)*, 871–878, DOI: <https://doi.org/10.1109/BigData.2015.7363835>. IEEE (IEEE, 2015).
26. Barbosa, H. *et al.* Uncovering the socioeconomic facets of human mobility. *Sci. Reports* **11**, 8616, DOI: <https://doi.org/10.1038/s41598-021-87407-4> (2021).
27. Oliver, N. *et al.* Mobile phone data for informing public health actions across the COVID-19 pandemic life cycle, DOI: <https://doi.org/10.1126/sciadv.abc0764> (2020).
28. Ubaldi, E. *et al.* Mobilkit: A Python Toolkit for Urban Resilience and Disaster Risk Management Analytics using High Frequency Human Mobility Data. *arXiv preprint arXiv:2107.14297* (2021). [2107.14297](https://doi.org/10.4236/arxiv.210714297).
29. Bengtsson, L. *et al.* Using Mobile Phone Data to Predict the Spatial Spread of Cholera. *Sci. Reports* **5**, 8923, DOI: <https://doi.org/10.1038/srep08923> (2015).
30. Peak, C. M. *et al.* Population mobility reductions associated with travel restrictions during the Ebola epidemic in Sierra Leone: use of mobile phone data. *Int. J. Epidemiol.* **47**, 1562–1570, DOI: <https://doi.org/10.1093/ije/dyy095> (2018).
31. Wesolowski, A. *et al.* Quantifying the Impact of Human Mobility on Malaria. *Science* **338**, 267–270, DOI: <https://doi.org/10.1126/science.1223467> (2012).
32. Chinazzi, M. *et al.* The effect of travel restrictions on the spread of the 2019 novel coronavirus (COVID-19) outbreak. *Science* **368**, 395–400, DOI: <https://doi.org/10.1126/science.aba9757> (2020).

33. Bonaccorsi, G. *et al.* Economic and social consequences of human mobility restrictions under COVID-19. *Proc. Natl. Acad. Sci.* **117**, 15530–15535, DOI: <https://doi.org/10.1073/pnas.2007658117> (2020).

34. Fraiberger, S. P. *et al.* Uncovering socioeconomic gaps in mobility reduction during the COVID-19 pandemic using location data. *arXiv preprint arXiv:2006.15195* (2020). [2006.15195](https://doi.org/10.4236/arxiv.200615195).

35. Xiong, C., Hu, S., Yang, M., Luo, W. & Zhang, L. Mobile device data reveal the dynamics in a positive relationship between human mobility and COVID-19 infections. *Proc. Natl. Acad. Sci.* **117**, 27087–27089, DOI: <https://doi.org/10.1073/pnas.2010836117> (2020).

36. Zhou, Y. *et al.* Effects of human mobility restrictions on the spread of COVID-19 in Shenzhen, China: a modelling study using mobile phone data. *The Lancet Digit. Heal.* **2**, e417–e424, DOI: [https://doi.org/10.1016/S2589-7500\(20\)30165-5](https://doi.org/10.1016/S2589-7500(20)30165-5) (2020).

37. da Silva, T. T., Francisquini, R. & Nascimento, M. C. Meteorological and human mobility data on predicting COVID-19 cases by a novel hybrid decomposition method with anomaly detection analysis: A case study in the capitals of Brazil. *Expert. Syst. with Appl.* **182**, 115190, DOI: <https://doi.org/10.1016/j.eswa.2021.115190> (2021).

38. Di Domenico, L., Pullano, G., Sabbatini, C. E., Boëlle, P.-Y. & Colizza, V. Impact of lockdown on COVID-19 epidemic in Île-de-France and possible exit strategies. *BMC Medicine* **18**, 240, DOI: <https://doi.org/10.1186/s12916-020-01698-4> (2020).

39. Klein, B. *et al.* Assessing changes in commuting and individual mobility in major metropolitan areas in the United States during the COVID-19 outbreak. Available from: <https://www.networkscienceinstitut> (2020).

40. Jones, A. *et al.* Impact of a Public Policy Restricting Staff Mobility Between Nursing Homes in Ontario, Canada During the COVID-19 Pandemic. *J. Am. Med. Dir. Assoc.* **22**, 494–497, DOI: <https://doi.org/10.1016/j.jamda.2021.01.068> (2021).

41. Wellenius, G. A. *et al.* Impacts of State-Level Policies on Social Distancing in the United States Using Aggregated Mobility Data during the COVID-19 Pandemic. *arXiv preprint arXiv:2004.10172* (2020). [2004.10172](https://doi.org/10.4236/arxiv.200410172).

42. Drake, T. M. *et al.* The effects of physical distancing on population mobility during the COVID-19 pandemic in the UK. *The Lancet Digit. Heal.* **2**, e385–e387, DOI: [https://doi.org/10.1016/S2589-7500\(20\)30134-5](https://doi.org/10.1016/S2589-7500(20)30134-5) (2020).

43. Dahlberg, M. *et al.* Effects of the COVID-19 Pandemic on Population Mobility under Mild Policies: Causal Evidence from Sweden. *arXiv preprint arXiv:2004.09087* (2020). [2004.09087](https://doi.org/10.4236/arxiv.200409087).

44. Yabe, T. *et al.* Non-compulsory measures sufficiently reduced human mobility in Tokyo during the COVID-19 epidemic. *Sci. Reports* **10**, 18053, DOI: <https://doi.org/10.1038/s41598-020-75033-5> (2020).

45. Schlosser, F. *et al.* COVID-19 lockdown induces disease-mitigating structural changes in mobility networks. *Proc. Natl. Acad. Sci.* **117**, 32883–32890, DOI: <https://doi.org/10.1073/pnas.2012326117> (2020).

46. Pullano, G., Valdano, E., Scarpa, N., Rubrichi, S. & Colizza, V. Evaluating the effect of demographic factors, socioeconomic factors, and risk aversion on mobility during the COVID-19 epidemic in France under lockdown: a population-based study. *The Lancet Digit. Heal.* **2**, e638–e649, DOI: [https://doi.org/10.1016/S2589-7500\(20\)30243-0](https://doi.org/10.1016/S2589-7500(20)30243-0) (2020).

47. Pepe, E. *et al.* COVID-19 outbreak response, a dataset to assess mobility changes in Italy following national lockdown. *Sci. Data* **7**, 230, DOI: <https://doi.org/10.1038/s41597-020-00575-2> (2020).

48. Showalter, E., Vigil-Hayes, M., Zegura, E., Sutton, R. & Belding, E. Tribal Mobility and COVID-19. In *Proceedings of the 22nd International Workshop on Mobile Computing Systems and Applications*, 99–105, DOI: <https://doi.org/10.1145/3446382.3448654> (ACM, New York, NY, USA, 2021).

49. Gozzi, N. *et al.* Estimating the effect of social inequalities on the mitigation of COVID-19 across communities in Santiago de Chile. *Nat. Commun.* **12**, 2429, DOI: <https://doi.org/10.1038/s41467-021-22601-6> (2021).

50. Bonato, P. *et al.* Mobile phone data analytics against the COVID-19 epidemics in Italy: flow diversity and local job markets during the national lockdown. *arXiv preprint arXiv:2004.11278* (2020). [2004.11278](https://doi.org/10.4236/arxiv.200411278).

51. Galeazzi, A. *et al.* Human mobility in response to COVID-19 in France, Italy and UK. *Sci. Reports* **11**, 13141, DOI: <https://doi.org/10.1038/s41598-021-92399-2> (2021).

52. Tizzoni, M. *et al.* On the Use of Human Mobility Proxies for Modeling Epidemics. *PLoS Comput. Biol.* **10**, e1003716, DOI: <https://doi.org/10.1371/journal.pcbi.1003716> (2014).

53. Hou, X. *et al.* Intracounty modeling of COVID-19 infection with human mobility: Assessing spatial heterogeneity with business traffic, age, and race. *Proc. Natl. Acad. Sci.* **118**, e2020524118, DOI: <https://doi.org/10.1073/pnas.2020524118> (2021).

54. Chang, S. *et al.* Mobility network models of COVID-19 explain inequities and inform reopening. *Nature* **589**, 82–87, DOI: <https://doi.org/10.1038/s41586-020-2923-3> (2021).

55. Weill, J. A., Stigler, M., Deschenes, O. & Springborn, M. R. Social distancing responses to COVID-19 emergency declarations strongly differentiated by income. *Proc. Natl. Acad. Sci.* **117**, 19658–19660, DOI: <https://doi.org/10.1073/pnas.2009412117> (2020).

56. Vaitla, B. *et al.* Big Data and the Well-Being of Women and Girls Applications on the Social Scientific Frontier. *Data2x* (2017).

57. Iio, K., Guo, X., Kong, X., Rees, K. & Bruce Wang, X. COVID-19 and social distancing: Disparities in mobility adaptation between income groups. *Transp. Res. Interdiscip. Perspectives* **10**, 100333, DOI: <https://doi.org/10.1016/j.trip.2021.100333> (2021).

58. Gao, S. Spatio-Temporal Analytics for Exploring Human Mobility Patterns and Urban Dynamics in the Mobile Age. *Spatial Cogn. & Comput.* **15**, 86–114, DOI: <https://doi.org/10.1080/13875868.2014.984300> (2015).

59. Hasan, S., Schneider, C. M., Ukkusuri, S. V. & González, M. C. Spatiotemporal Patterns of Urban Human Mobility. *J. Stat. Phys.* **151**, 304–318, DOI: <https://doi.org/10.1007/s10955-012-0645-0> (2013).

60. González, M. C., Hidalgo, C. A. & Barabási, A.-L. Understanding individual human mobility patterns. *Nature* **458**, 238–238, DOI: <https://doi.org/10.1038/nature07850> (2009).

61. Song, C., Koren, T., Wang, P. & Barabási, A.-L. Modelling the scaling properties of human mobility. *Nat. Phys.* **6**, 818–823, DOI: <https://doi.org/10.1038/nphys1760> (2010).

62. Chung, H., Birkett, H., Forbes, S. & Seo, H. Covid-19, Flexible Working, and Implications for Gender Equality in the United Kingdom. *Gend. & Soc.* **35**, 218–232, DOI: <https://doi.org/10.1177/08912432211001304> (2021).

63. ONS. Coronavirus and homeworking in the UK labour market. *Off. for Natl. Stat.* (2020).

64. Alessandretti, L., Aslak, U. & Lehmann, S. The scales of human mobility. *Nature* **587**, 402–407, DOI: <https://doi.org/10.1038/s41586-020-2909-1> (2020).

65. Morgan, M. A. & Berry, B. J. L. *Geography of Market Centers and Retail Distribution*, vol. 134 (Englewood Cliffs, NJ: Prentice-Hall, 1968).

66. Kishore, N. *et al.* Lockdowns result in changes in human mobility which may impact the epidemiologic dynamics of SARS-CoV-2. *Sci. Reports* **11**, 6995, DOI: <https://doi.org/10.1038/s41598-021-86297-w> (2021).

67. Sigler, T. *et al.* The socio-spatial determinants of COVID-19 diffusion: the impact of globalisation, settlement characteristics and population. *Glob. Heal.* **17**, 56, DOI: <https://doi.org/10.1186/s12992-021-00707-2> (2021).

68. Neiderud, C.-J. How urbanization affects the epidemiology of emerging infectious diseases. *Infect. Ecol. & Epidemiol.* **5**, 27060, DOI: <https://doi.org/10.3402/iee.v5.27060> (2015).

69. Ali, S. H. & Keil, R. Global Cities and the Spread of Infectious Disease: The Case of Severe Acute Respiratory Syndrome (SARS) in Toronto, Canada. *Urban Stud.* **43**, 491–509, DOI: <https://doi.org/10.1080/00420980500452458> (2006).

70. Pateman, T. Rural and urban areas: comparing lives using rural/urban classifications. *Reg. Trends* **43**, 11–86, DOI: <https://doi.org/10.1057/rt.2011.2> (2011).

71. Huang, Q. *et al.* Urban-rural differences in COVID-19 exposures and outcomes in the South: A preliminary analysis of South Carolina. *PLOS ONE* **16**, e0246548, DOI: <https://doi.org/10.1371/journal.pone.0246548> (2021).

72. Khavarian-Garmsir, A. R., Sharifi, A. & Moradpour, N. Are high-density districts more vulnerable to the COVID-19 pandemic? *Sustain. Cities Soc.* **70**, 102911, DOI: <https://doi.org/10.1016/j.scs.2021.102911> (2021).

73. Kutela, B., Novat, N. & Langa, N. Exploring geographical distribution of transportation research themes related to COVID-19 using text network approach. *Sustain. Cities Soc.* **67**, 102729, DOI: <https://doi.org/10.1016/j.scs.2021.102729> (2021).

74. Lee, M. *et al.* Human mobility trends during the early stage of the COVID-19 pandemic in the United States. *PLOS ONE* **15**, e0241468, DOI: <https://doi.org/10.1371/journal.pone.0241468> (2020).

75. Lenormand, M. *et al.* Influence of sociodemographic characteristics on human mobility. *Sci. Reports* **5**, 10075, DOI: <https://doi.org/10.1038/srep10075> (2015).

76. Hariharan, R. & Toyama, K. Project Lachesis: Parsing and Modeling Location Histories. In *Lecture Notes in Computer Science (including subseries Lecture Notes in Artificial Intelligence and Lecture Notes in Bioinformatics)*, vol. 3234, 106–124, DOI: https://doi.org/10.1007/978-3-540-30231-5_8 (Nature Publishing Group, 2004).

77. Office for National Statistics. Income estimates for small areas, England and Wales (2020).
78. Chandola, T. & Jenkinson, C. The new UK national statistics socio-economic classification (NS-SEC); investigating social class differences in self-reported health status. *J. Public Heal.* **22**, 182–190, DOI: <https://doi.org/10.1093/pubmed/22.2.182> (2000).
79. Office for National Statistics. *2011 Census: Aggregate Data (Edition: June 2016)* (InFuse, 2020).
80. Toole, J. L., Ulm, M., González, M. C. & Bauer, D. Inferring land use from mobile phone activity. In *Proceedings of the ACM SIGKDD International Workshop on Urban Computing - UrbComp '12*, 1, DOI: <https://doi.org/10.1145/2346496.2346498> (ACM Press, New York, New York, USA, 2012).
81. VanderPlas, J. T. Understanding the Lomb–Scargle Periodogram. *The Astrophys. J. Suppl. Ser.* **236**, 16, DOI: <https://doi.org/10.3847/1538-4365/aab766> (2018).

Acknowledgements

This work is a collaboration between the Department of Computer Science of the University of Exeter and Cuebiq Inc. In response to the COVID-19 crisis, [Cuebiq](#) is providing insights to academic and humanitarian groups through a multi-stakeholder [data collaborative](#) for timely and ethical analysis of aggregate human mobility patterns. This manuscript is the outcome of this collaboration Cuebiq Inc and summarises the main findings. Besides this paper, two additional, non-peer reviewed, reports were produced during the first national lockdown with an initial analysis of the pandemic in the UK and a second one with analysing changes in socio-economic aspects related to mobility patterns in the UK during the first lockdown. Both reports are available at the project web page covid19-uk-mobility.github.io.

Author contributions statement

CS performed the analysis. RDC and FP gather the data. RDC, FB, HB, RM designed the analysis. CS and RDC wrote the paper. RM, RDC supervised the project. All authors discussed the results and contributed to the final manuscript.

Competing interests

The authors declare no competing interests.

Additional information

Additional information for this paper is also available at <https://covid19-uk-mobility.github.io>

Correspondence and requests for materials should be addressed to RDC.

Supplementary Materials

S1 Data Information

Column	Description
year	Year when the location information was saved in the database
week	Week number according to the ISO-8601 standard where weeks start on Monday. It is a number between 1 and 52 (or 53 for leap years)
radius	The average radius of gyration in kilometres for the users inside a region at a given week of the year. The values were normalised using a min-max normalisation to comply with data sharing policies
pings	Represents the number of pings (sync connections sent from the users' devices to the data server). The values were also normalised using a min-max normalisation to comply with data sharing policies
geo_code	Unique codes for local authority districts (LAD) and unitary authorities (UA) in the United Kingdom

Table S1.1. Description of the data used to analyse the spatial dimension of mobility, i.e. radius of gyration.

Column	Description
year	Year when the location information was saved in the database
day	Number between 1 and 365 (or 366 for leap years) where January 1 is day 1. This indicates the day when the out-of-home event was identified
hour	Integer between 0 and 24 which represents the hour when the Out-of-Home event was identified
trips	Total number of times that the users in a given area left home at a given period of time, i.e., the number of Out-of-home trips. The values were normalised using a min-max normalisation to comply with data sharing policies
geo_code	Unique codes for local authority districts (LAD) and unitary authorities (UA) in the United Kingdom

Table S1.2. Description of the data used to analyse the temporal dimension of mobility, i.e. mobility synchronisation.

In Figure S1.1 each point represents a local authority colour-coded by their country, and the axis represents the number of users and the population as a percentage of the total. A strong positive correlation between the populations compared is observed in Figure S1.1 with r^2 value of 0.78.

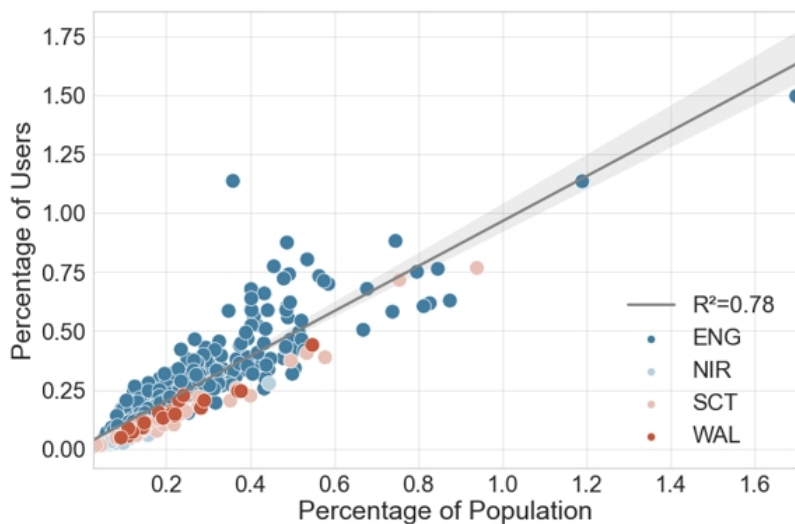


Figure S1.1. Correlation between the percentage of users and the population. Each point in the scatter plot represents a local authority in the UK, and the colour indicates its country. The x-axis represents the division of the region's population by the sum of the population of all regions. Similarly, the y-axis represents the number of users in a local authority divided by the total number of users in the data.

S2 NS-SEC Classification

The urban-rural classification adopted for England⁷⁰ has two levels of classification. The first level classifies areas as urban, rural and urban with significant rural, while the second level classifies the areas into six levels of urbanisation ranging from level 1 to level 6. Level 1 corresponds to rural areas or low urbanisation index, while level 6 describes areas classified as major urban or high-urbanisation indexes. Table S2.3 summarises the NS-SEC classes used in our analysis.

Class	Description
NS-SEC 1	Higher managerial, administrative and professional occupations
NS-SEC 2	Lower managerial, administrative and professional occupations
NS-SEC 3	Intermediate occupations (e.g. Intermediate clerical, administrative, sales, service, engineering, technical and auxiliary occupations)
NS-SEC 4	Small employers and own account workers
NS-SEC 5	Lower supervisory and technical occupations
NS-SEC 6	Semi-routine occupations
NS-SEC 7	Routine occupations
NS-SEC 8	Never worked and long-term unemployed

Table S2.3. The National Statistics Socio-economic classification (NS-SEC) classes description.

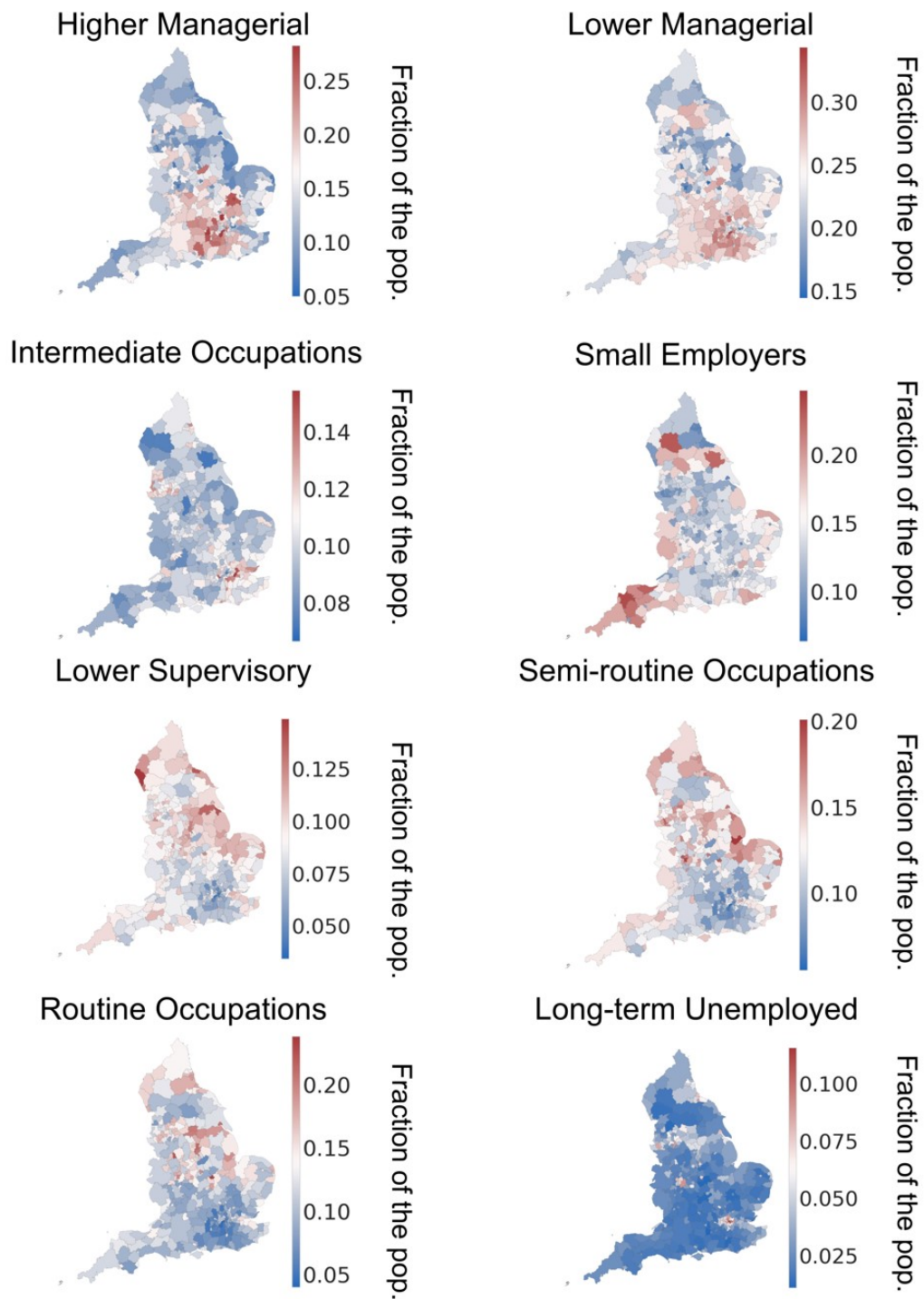


Figure S2.2. Fraction of the local authorities' population in the NS-SEC classes studied.

S3 Spatio-temporal Metrics

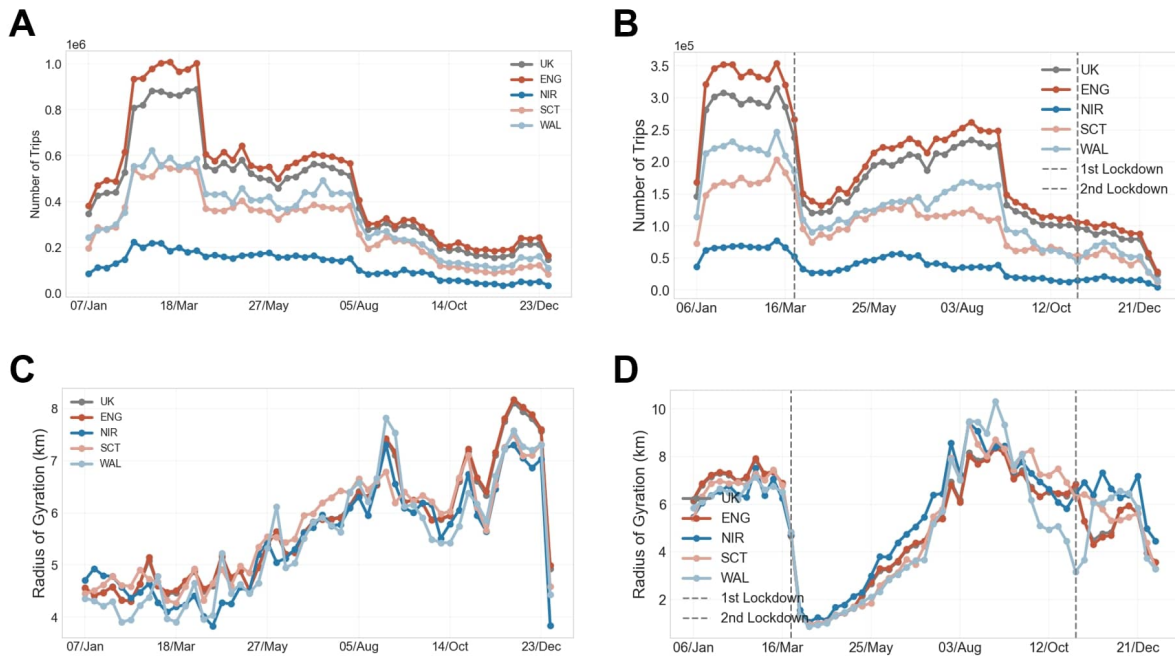


Figure S3.3. Evolution of the radius of gyration (A) and number of out-of-home trips (B) in 2020 for the UK and its countries. (C) presents the comparison of the radius of gyration in 2019 and 2020 for the UK. Note that the 2020 radius of gyration values continued the trend interrupted by the lockdown effect in the middle of March at the end of July.

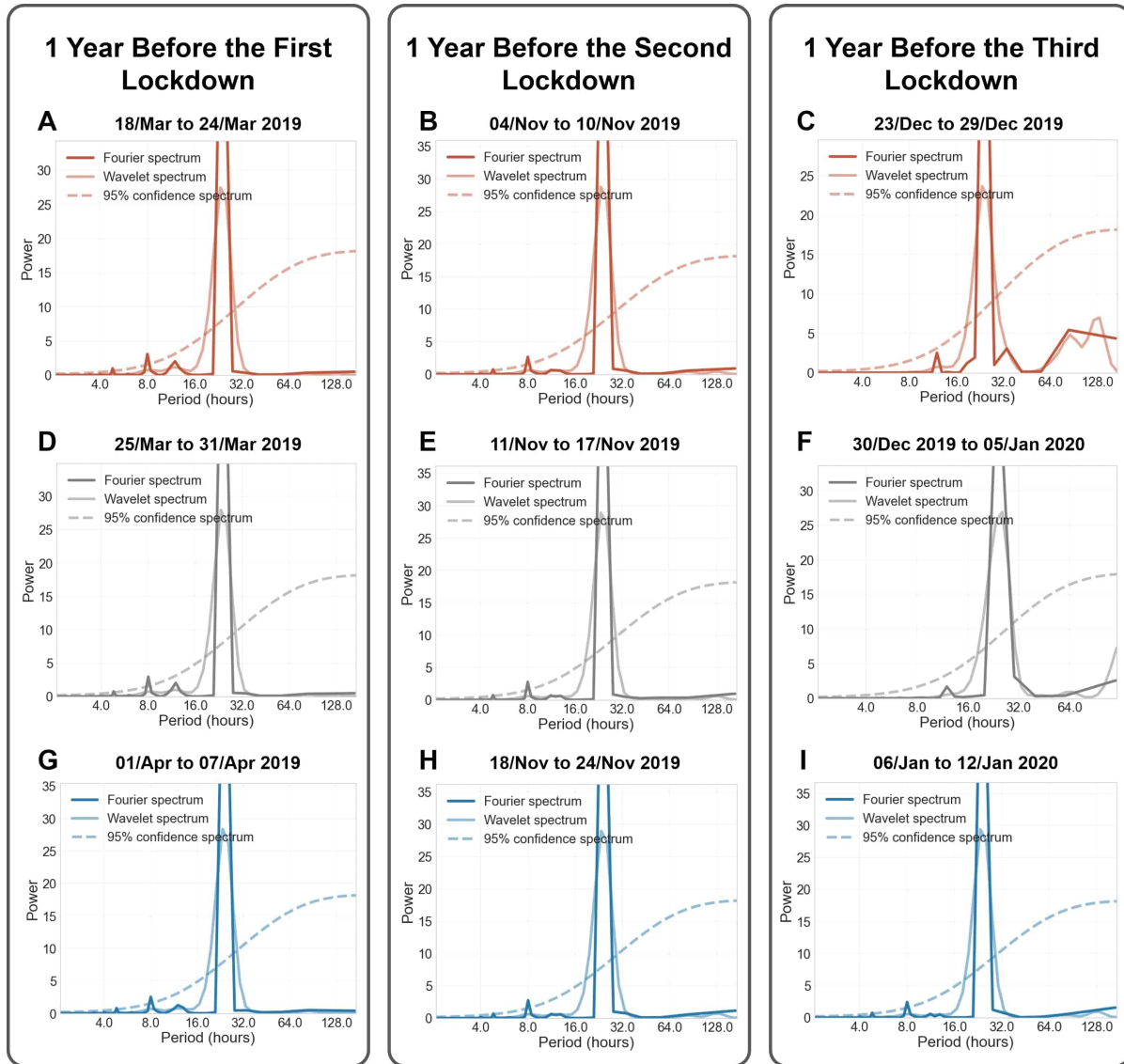


Figure S3.4. Assessment of the mobility synchronisation periods for the baseline year (i.e. 2019 and January 2020). Panels A, B and C represent the patterns for the baseline period corresponding to the week before the announcement of the lockdowns. Panels D, E and F depict the baseline week's patterns when the lockdowns were announced. Lastly, panels G, H and I show the baseline patterns for the week corresponding to the second week of lockdown. The synchronisation periods above the 95% confidence interval is based on the global wavelet and Fourier for the *out-of-home* trips spectra on ea, ch period. Note that, in the baseline, the most significant periods are t, o the, and 24hrs. However, since the 24hrs components dominate the other, it was not considered for calculating the mobility synchronisation metric.

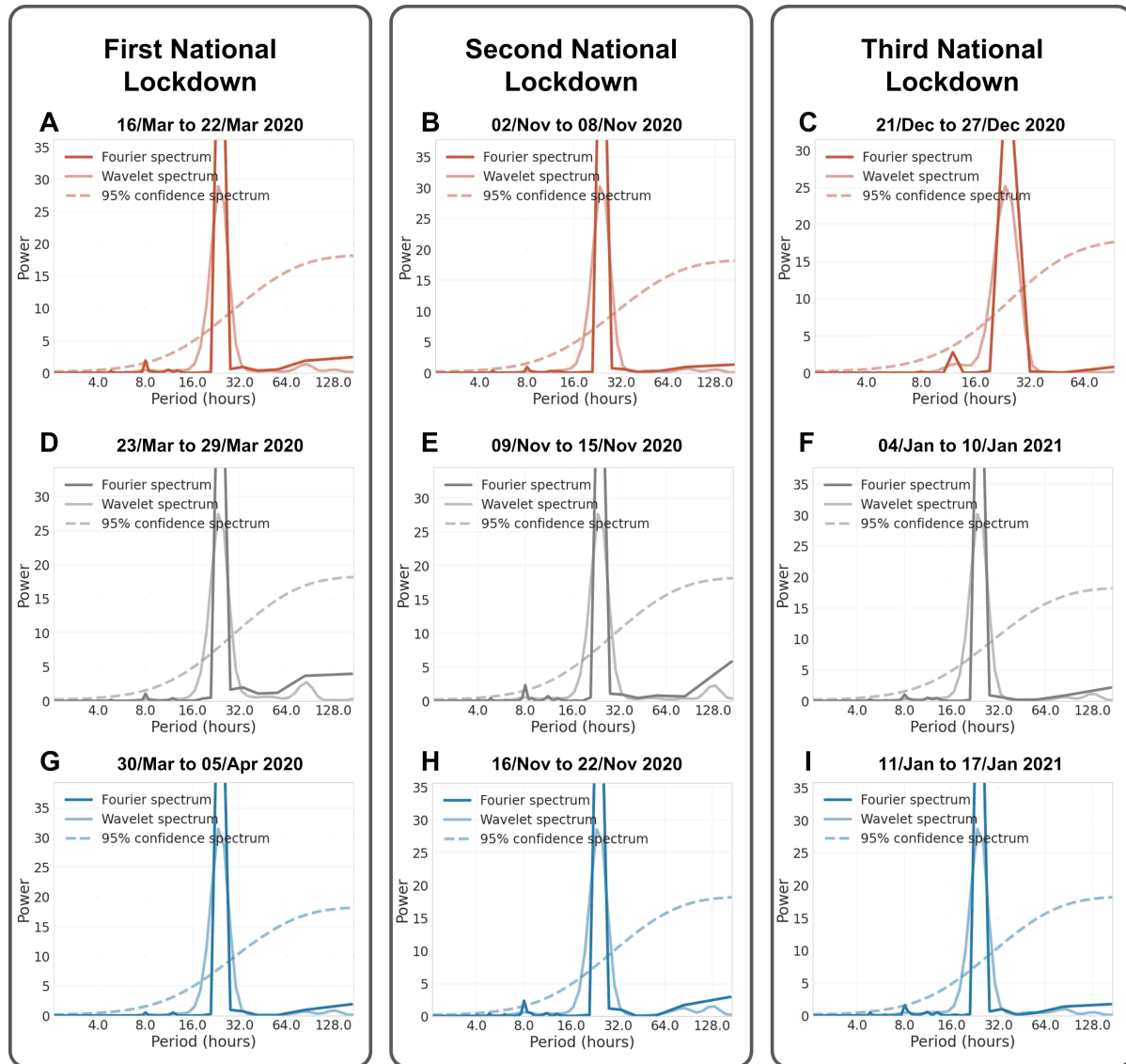


Figure S3.5. Assessment of the mobility synchronisation in the UK before the national lockdowns (A, B, and C), in the first week of the lockdowns (D, E and F), and in the second week of the lockdowns (G and H). The synchronisation periods above the 95% confidence interval is based on the global wavelet and Fourier for the *out-of-home* trips spectra on each period. Note that the synchronisation pattern was mostly changed during the lockdown period as (D) and (E) show a reduction in the spike at 8hrs mark when compared to the period before first lockdown (A).

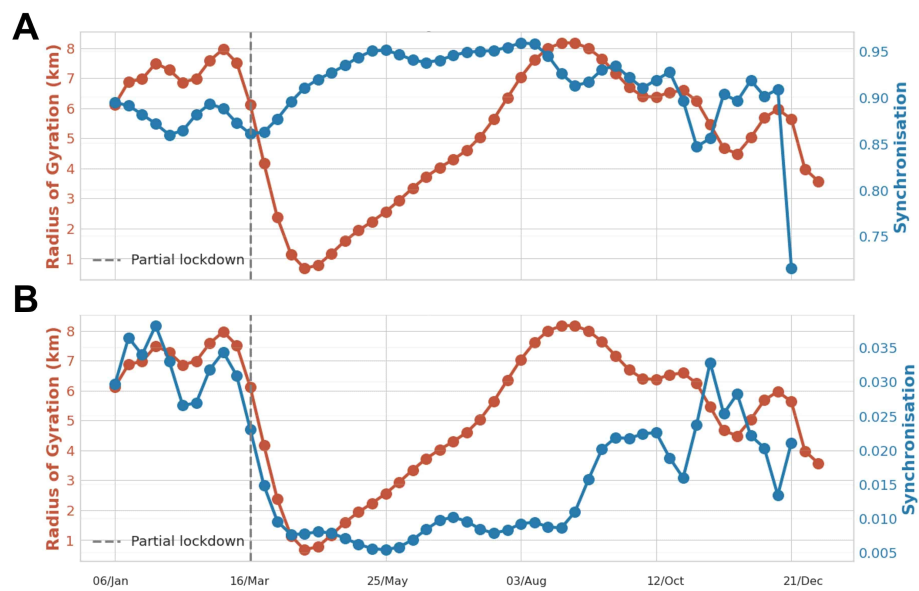


Figure S3.6. Comparison between the Spatio-temporal dimensions of mobility. Panel A shows the calculation of the mobility synchronisation metric using the 24hrs components, while B depicts the behaviour of this metric without it (B). Note the similarities in the trends of both metrics in Panel B for the period before the first lockdown.

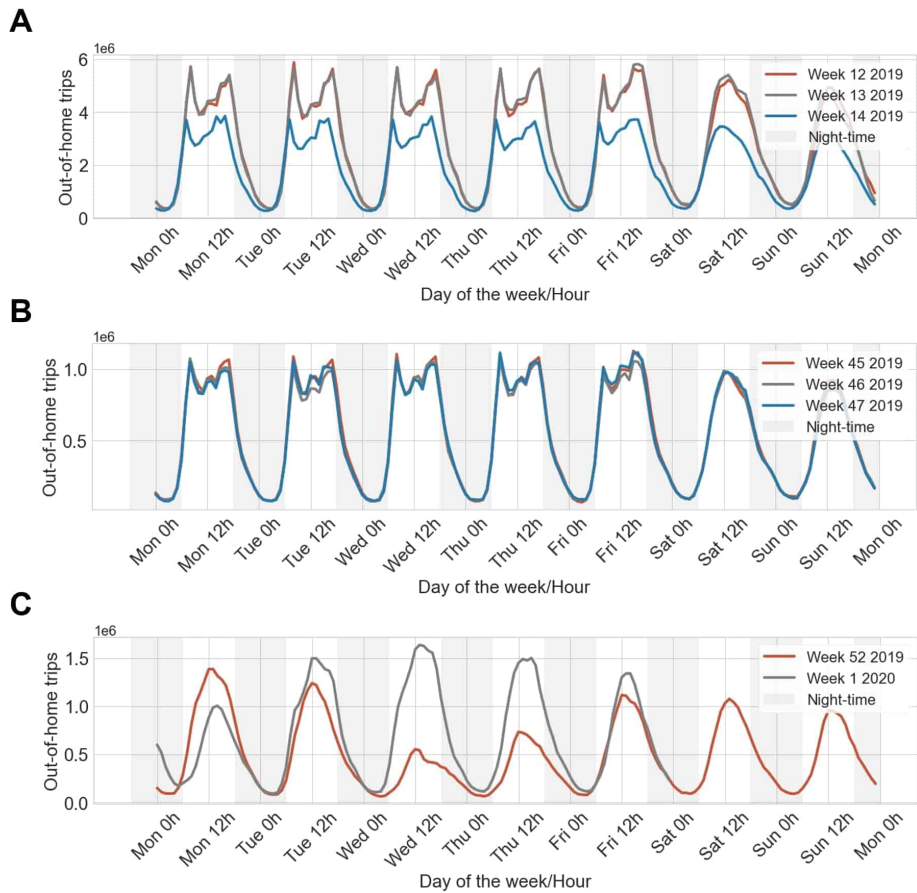


Figure S3.7. Comparison of the number of out-of-home trips in the same periods depicted by Figure S3.4 for the first lockdown (L1), second lockdown (L2) and third lockdown (L3). The results presented in this figure supports the results in Figure S3.4. We can see that the waves for the first lockdown period (A) presents a reduced magnitude (fewer people leaving home) and loses the multiple peaks present in the week before L1.

S4 Mobility Patterns in England

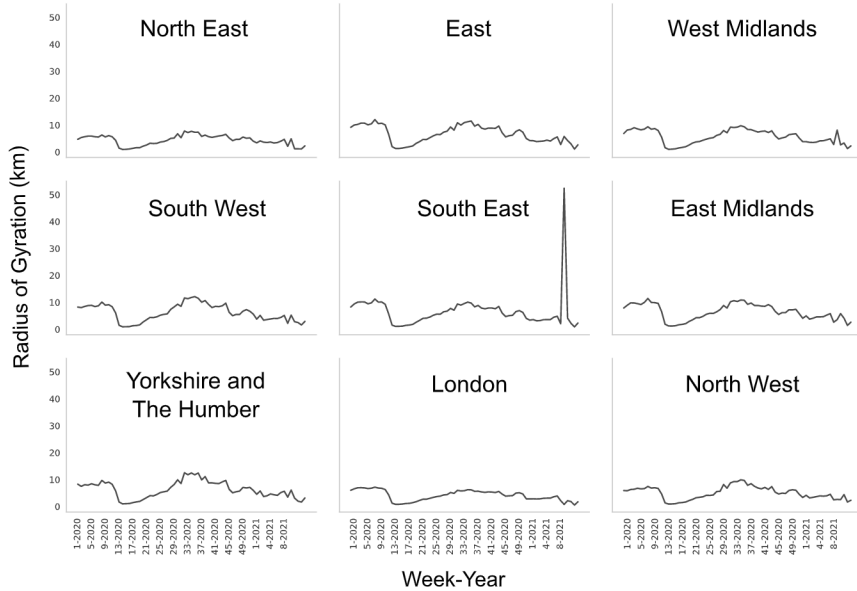


Figure S4.8. Radius of gyration time series for the regions in England. Period from week 1 2020 until week 8 2021.

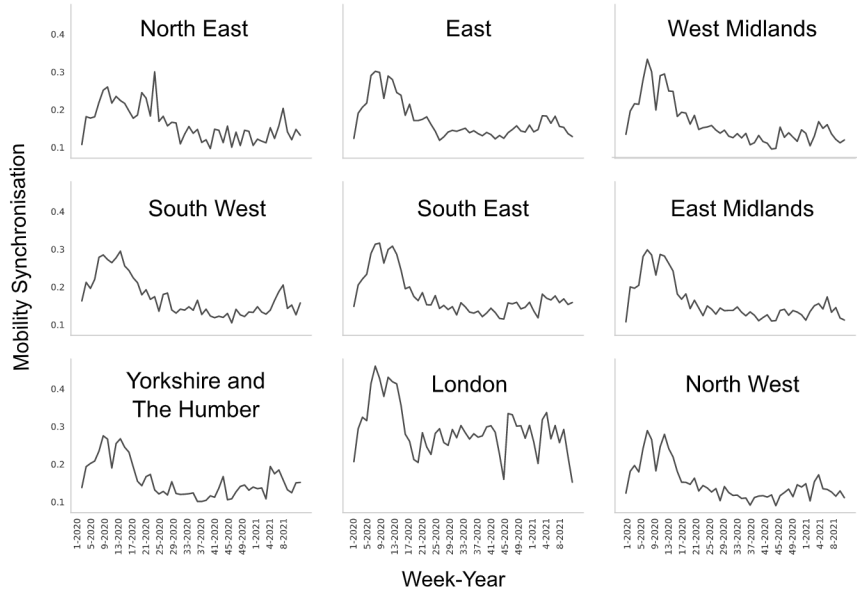


Figure S4.9. Mobility synchronisation time series for the regions in England. Period from week 1 2020 until week 8 2021.

S5 Mobility Patterns in Northern Ireland

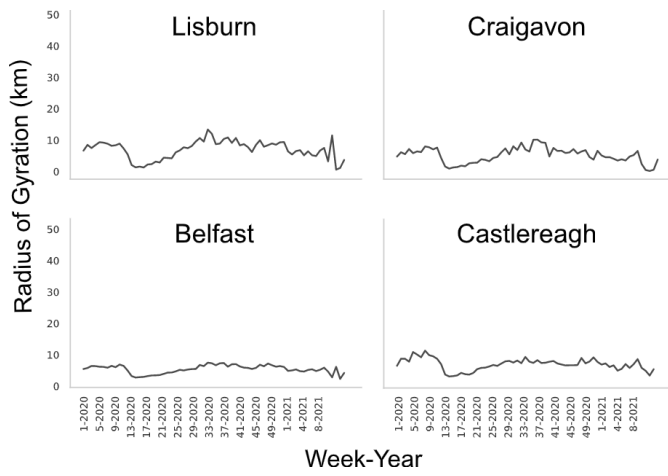


Figure S5.10. Radius of gyration time series for the studied areas in Northern Ireland. Period from week 1 2020 until week 8 2021.

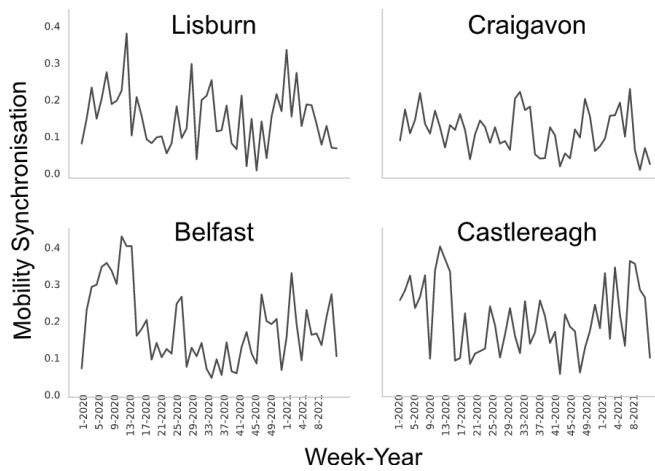


Figure S5.11. Mobility synchronisation time series for the studied areas in Northern Ireland. Period from week 1 2020 until week 8 2021.

S6 Mobility Patterns in Scotland

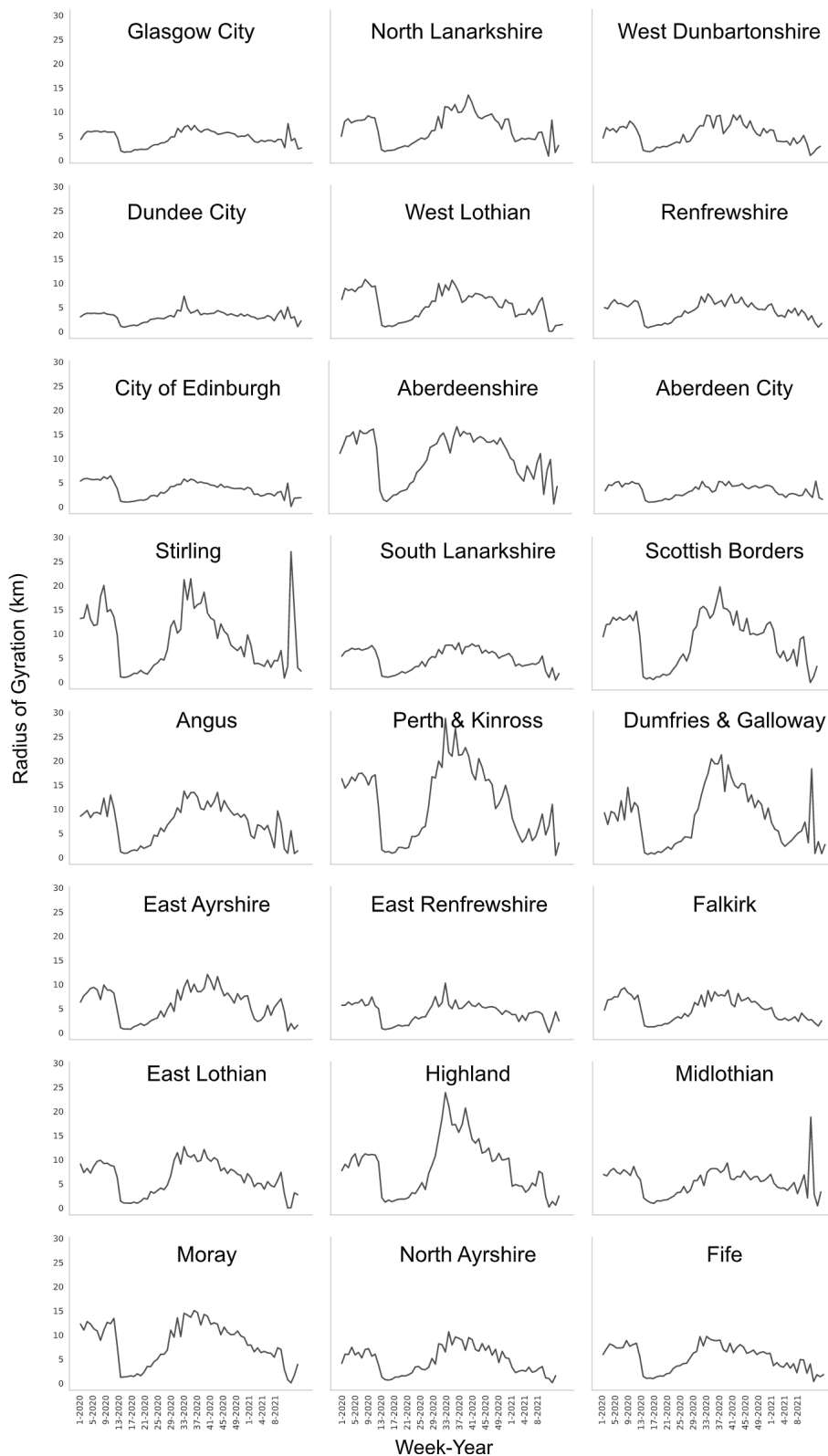


Figure S6.12. Radius of gyration time series for the studied areas in Scotland. Period from week 1 2020 until week 8 2021.

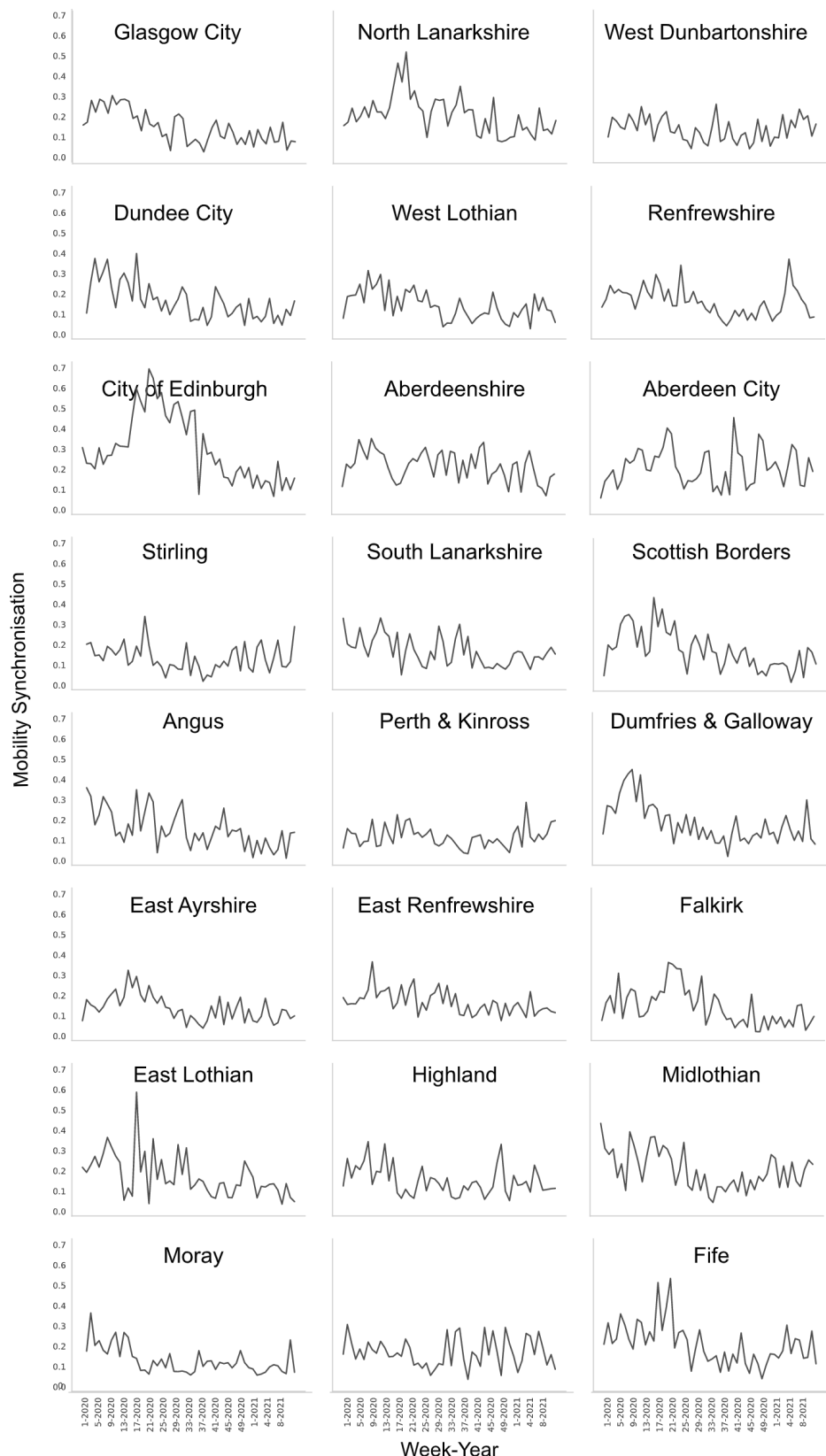


Figure S6.13. Mobility synchronisation time series for the studied areas in Scotland. Period from week 1 2020 until week 8 2021.

S7 Mobility Patterns in Wales

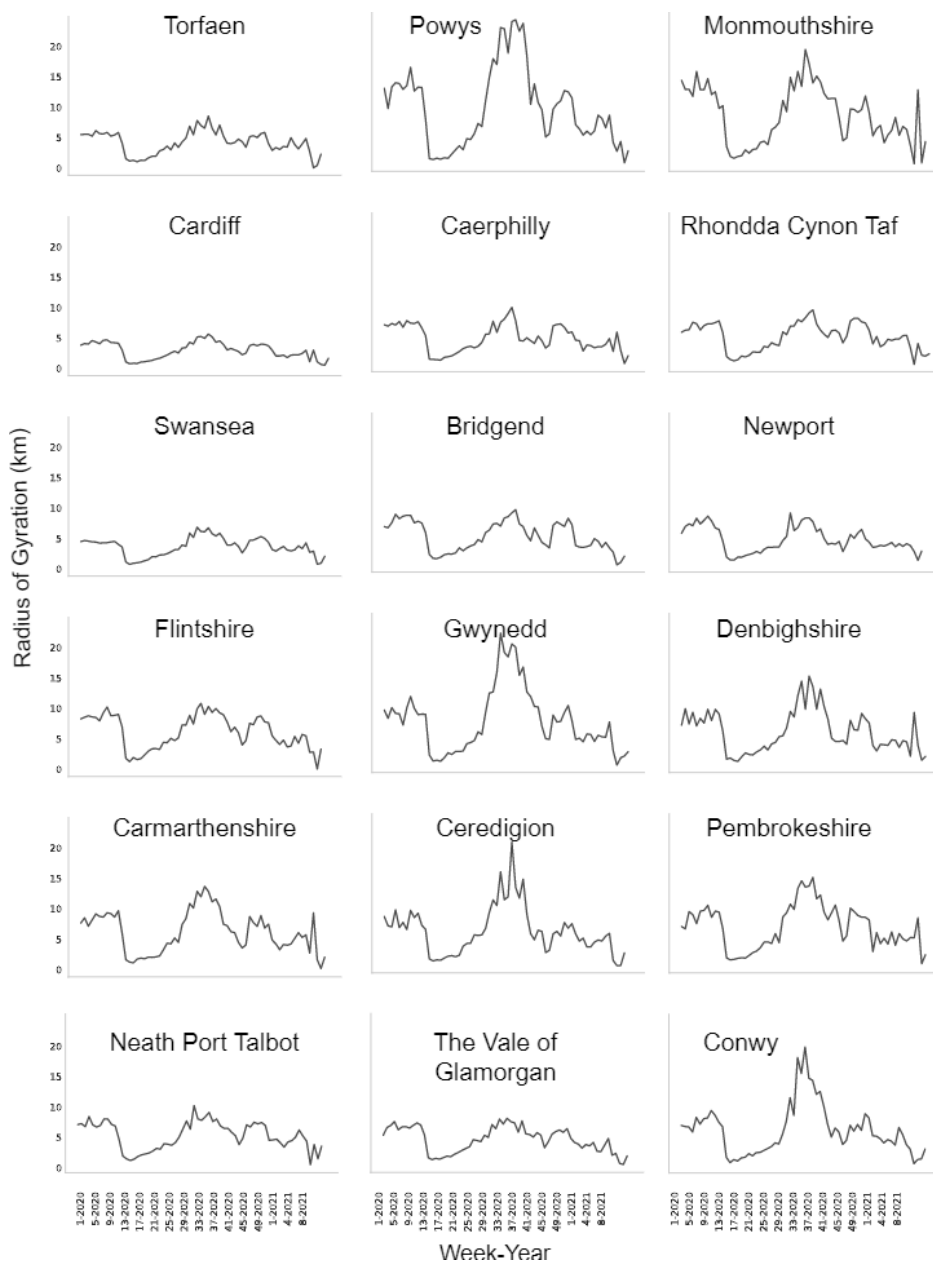


Figure S7.14. Radius of gyration time series for the studied areas in Wales. Period from week 1 2020 until week 8 2021.

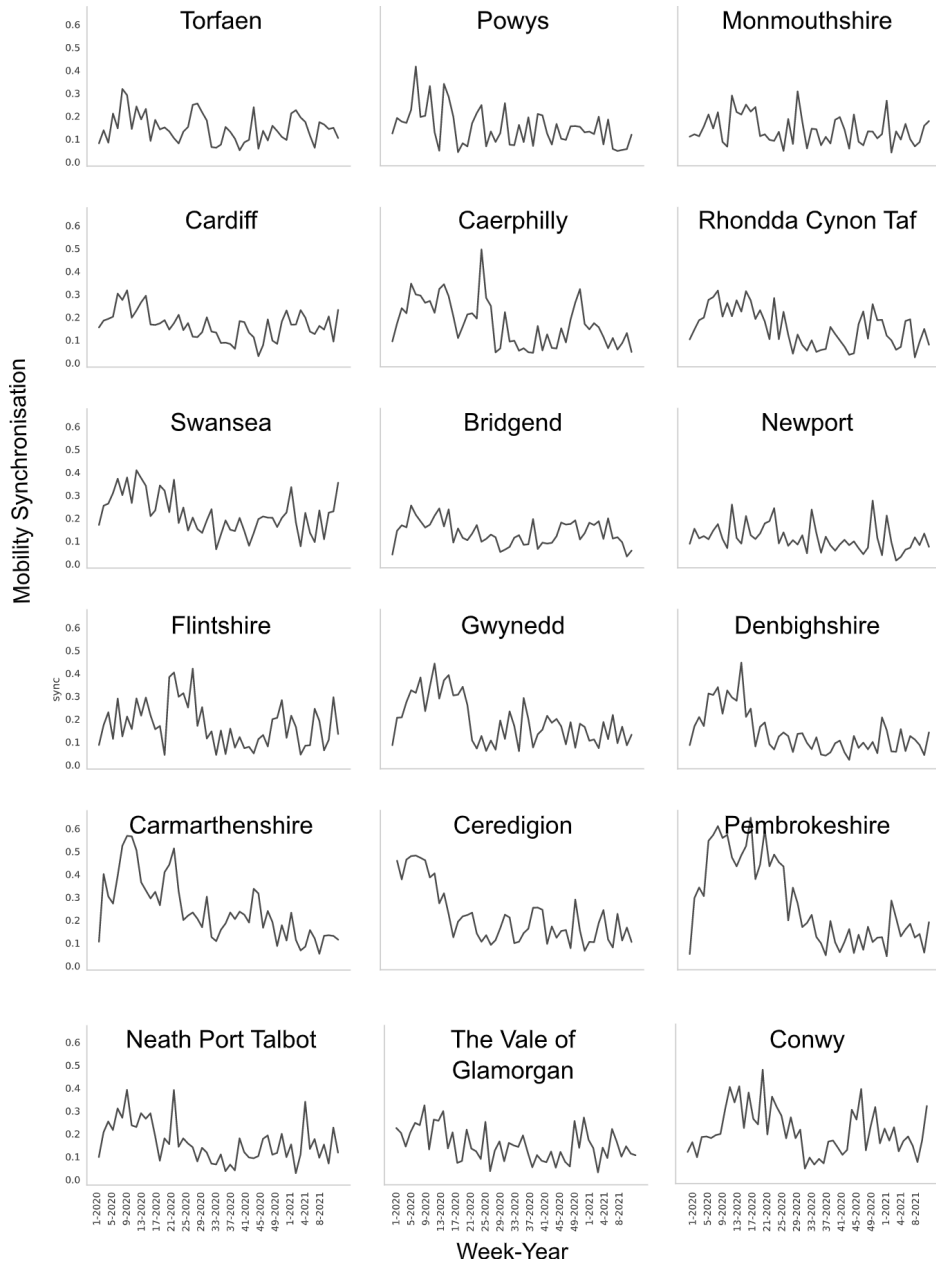


Figure S7.15. Mobility synchronisation time series for the studied areas in Wales. Period from week 1 2020 until week 8 2021.